



**HAL**  
open science

## Viscoelastic effects in fingering between miscible fluids

H. van Damme, C. Laroche, L. Gatineau, P. Levitz

► **To cite this version:**

H. van Damme, C. Laroche, L. Gatineau, P. Levitz. Viscoelastic effects in fingering between miscible fluids. *Journal de Physique*, 1987, 48 (7), pp.1121-1133. 10.1051/jphys:019870048070112100 . jpa-00210533

**HAL Id: jpa-00210533**

**<https://hal.science/jpa-00210533>**

Submitted on 4 Feb 2008

**HAL** is a multi-disciplinary open access archive for the deposit and dissemination of scientific research documents, whether they are published or not. The documents may come from teaching and research institutions in France or abroad, or from public or private research centers.

L'archive ouverte pluridisciplinaire **HAL**, est destinée au dépôt et à la diffusion de documents scientifiques de niveau recherche, publiés ou non, émanant des établissements d'enseignement et de recherche français ou étrangers, des laboratoires publics ou privés.

Classification  
 Physics Abstracts  
 47.20 — 68.10

## Viscoelastic effects in fingering between miscible fluids

H. Van Damme, C. Laroche, L. Gatineau and P. Levitz

Centre de Recherche sur les Solides à Organisation Cristalline Imparfaites,  
 1B, rue de la Férellerie, 45071 Orléans Cedex 02, France

(Reçu le 29 décembre 1986, révisé le 24 mars 1987, accepté le 27 mars 1987)

**Résumé.** — Nous avons étudié les digitations formées par de l'eau injectée dans des suspensions aqueuses concentrées (des pâtes) d'argiles, dans le but d'établir les relations entre les propriétés viscoélastiques de la pâte et les trois caractéristiques suivantes des digitations : la largeur moyenne des « doigts », leur profil, et l'angle moyen de branchement. Le résultat principal est que le module d'élasticité de la pâte,  $G$  (approximé par le seuil d'écoulement,  $\sigma_0$ ) est un paramètre-clé dans ces relations. Lorsque l'on augmente la concentration de la pâte, dans un domaine de rapport solide/liquide allant de 0,05 à 0,10 en poids, on observe : (i) une augmentation spectaculaire de  $\sigma_0$  (donc de  $G$ ) allant de  $\sim 1,5$  Pa à  $\sim 140$  Pa ; (ii) une décroissance de la largeur moyenne des doigts, suivant une loi de puissance en  $\sigma_0^{-0,25}$  ; (iii) un changement radical de la courbure des doigts et surtout des fronts de doigts qui, de convexes, deviennent concaves. Cette courbure concave pourrait correspondre, soit à une singularité prédite par Shraiman et Bensimon, soit, plus vraisemblablement, à l'apparition de phénomènes de fracture ; (iv) une ouverture progressive de l'angle de branchement  $\beta$  jusqu'à  $\beta = \pi/2$  et une *asymétrisation* des branchements. L'ensemble des résultats suggère que la structure fortement branchée des figures de digitation en milieu viscoélastique est contrôlée pour une large part par les propriétés élastiques. Le mécanisme de branchement pourrait être associé à des cycles d'accélération et de ralentissement du front, en permanence autour d'une réponse élastique.

**Abstract.** — Fingering of water injected in concentrated suspensions of clay particles in water (pastes) has been studied in Hele Shaw channels with the aim of investigating the relationships of the paste viscoelastic properties with three fingers characteristics : the average finger width, the finger profile and the branching angle. The main result is that the elastic modulus,  $G$ , approximated by the yield stress,  $\sigma_0$ , of the paste is a key parameter in these relationships. Increasing the solid/liquid (weight by weight) ratio in the paste from 0.05 to 0.10 leads (i) to a dramatic rise of  $\sigma_0$ , from  $\sim 1.5$  Pa to  $\sim 140$  Pa ; (ii) to a decrease of the average finger width, according to a  $\sigma_0^{-0,25}$  power law ; (iii) to an abrupt change of the tips profile — from convex to concave — which can be rationalized either in terms of the cusp singularity predicted by Shraiman and Bensimon in the zero surface tension limit, or, more likely, in terms of the onset of fracture phenomena ; (iv) to an opening of the average branching angle  $\beta$  up to  $\beta = \pi/2$  and to the development of *asymmetric* branching. When taken together, the results suggest that the highly branched structure of viscoelastic fingers is controlled to a large extent by the elastic properties of the pushed medium, the elastic response limiting the speed of the tips. Branching might be associated to fluctuations close to this limit.

### 1. Introduction.

The hydrodynamic instability which characterizes the flow of a low viscosity fluid pushing a more viscous fluid into a Hele-Shaw channel can lead to two extreme pattern growth processes : Saffman-Taylor fingering [1] on the one hand, which is characterized, after a short transient, by a single and smooth finger moving steadily through the channel, and fractal fingering [2] on the other hand, which is characterized, from the very beginning of the flow, by extensively branched fingers. Experimentally,

Saffman-Taylor fingering is observed with immiscible Newtonian fluids having a non-negligible surface tension, whereas fractal fingering has been observed with miscible fluids, the more viscous one being non Newtonian (shear-thinning).

After about thirty years of experimental [1, 3] and theoretical [4] efforts, Saffman-Taylor flow is now pretty well understood. In particular, the mechanism leading to the selection of one finger size  $\lambda = l/w$  ( $l$  is the finger width,  $w$  is the channel width) for a given value of the control parameter  $1/B^* =$

$12 \mu U w^2 / T^* b^2$  ( $\mu$  is the viscosity of the more viscous fluid;  $U$  is the tip velocity;  $T^*$  is the effective surface tension;  $b$  is the cell thickness), as well as the asymptotic limit of the finger size at high velocity ( $\lambda = 1/2$ ) is now clear.

Fractal fingering is still far from offering such a consistent picture. Most of the efforts have been directed towards a description of the growth process in conditions leading to DLA type patterns [5-8], in radial cells. We have recently broadened the picture by showing that a whole family of fractal dimensions for growth can be obtained by changing the viscosity and the injection pressure, the resulting tip velocity being a reasonably good control parameter [9]. We also showed that the velocity dependence of the displacement efficiency,  $\delta$  ( $\delta$  is the fractional volume of the more viscous fluid displaced by the less viscous fluid), is dominated by the tip-splitting cascade of the fingers, and not by major changes of the average finger width,  $\bar{l}$ .  $\bar{l}$  was found to decrease slightly with increasing tip velocity.

The purpose of this paper is to report a brief experimental study of the finger properties (width, curvature, orientation) in Hele-Shaw channels, focusing on the influence of the viscoelastic properties of the medium. This is an important point since all the fluids which were used to study fractal fingering up to now (polymer solution [2, 5-7], suspensions of latex spheres [5], suspensions of clay particles [8, 9]) are in fact colloidal viscoelastic media. We used colloidal clay suspensions and pastes.

The first part of the paper will be devoted to the relationships between the fingerwidth and three parameters: the cell thickness,  $b$ ; the injection pressure  $P_i$ , and the paste concentration.

In the second part, we wish to report some data about an aspect of fractal fingering which was not addressed so far: the finger and the tip profile. As we shall see, using miscible fluids leads to profiles which are fundamentally different from those observed in Saffman-Taylor flow. Experimental evidence for cusp shaped fingers will be presented for the first time.

Finally, we will briefly analyse the relationship between branching angle and paste rigidity.

All the data that we have suggest that the finger characteristics are controlled by the elastic rather than the viscous properties of the displaced fluid.

## 2. Experimental.

As in our previous work, we used water as the less viscous fluid and concentrated suspensions (pastes) of clay particles (Wyoming bentonite from N.L. Industries) as the more viscous fluids. The solid/water ratio in the paste,  $S/L$ , was between 0.05 and 0.10 (weight by weight). Bentonite pastes are viscoelastic shear-thinning materials with a threshold

for flow (the yield stress,  $\sigma_0$ ). As shown in figure 1, their rheological behaviour is well described by a generalized Casson equation [10]:

$$(\sigma - \sigma_0) \sim \dot{\gamma}^m \quad (1)$$

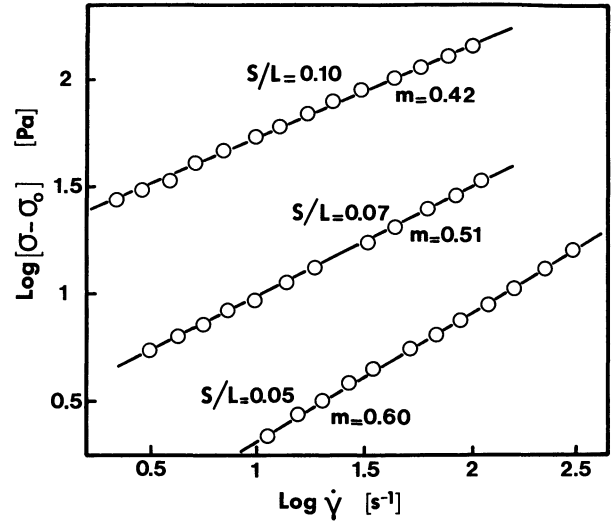


Fig. 1. — Rheological behaviour of the clay pastes plotted according to a generalized Casson equation (Eq. (1) in text).  $S/L$  is the clay to water ratio (w/w) in the paste. A typical flow curve, with the yield stress,  $\sigma_0$ , and the Bingham yield value,  $\sigma_B$ , is shown in the insert of figure 2.

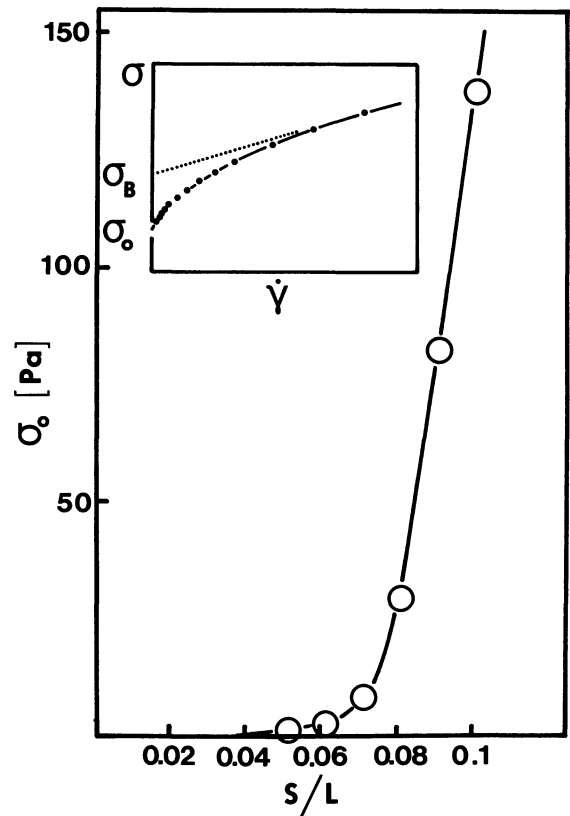


Fig. 2. — Concentration dependence of the yield stress in the clay pastes.

where  $\sigma$  is the shear stress and  $\dot{\gamma}$  the shear rate (velocity gradient). The shear-thinning exponent,  $m$ , is a decreasing function of  $S/L$  whereas  $\sigma_0$  is a steeply increasing function of  $S/L$  (Fig. 2). This expresses the development of the elastic properties. Also interesting in this respect is the extrapolated yield stress (the so-called Bingham yield value),  $\sigma_B$ , obtained by extrapolating the quasi-linear high shear stress region of the flow curves to zero shear rate (Fig. 2, insert). The pastes were prepared and characterized as described elsewhere [9]. The numerical values of  $m$  and  $\sigma_0$  and  $\sigma_B$  are collected in table I.

A horizontal cell of dimension  $1\text{ m} \times 0,3\text{ m} \times b$  was used, with copper spacers and rubber joints.

Table I. — Rheological parameters of the clay pastes.

S/L	0.05	0.06	0.07	0.08	0.09	0.10
$\sigma_0$ (Pa)	1.6	3	8	30	82	137
$m$	0.60	0.55	0.51	0.48	0.45	0.42
$\sigma_B$ (Pa)	6	12	25	57	130	220

$S/L$  is the clay to water ratio (weight by weight) in the paste.  
 $\sigma_0$  is the yield stress.  
 $\sigma_B$  is the Bingham yield value.  
 $m$  is the shear-thinning exponent used in equation (1) :  
 $(\sigma - \sigma_0) \sim \dot{\gamma}^m$ .  
 $\sigma$  is the shear stress.  
 $\dot{\gamma}$  is the shear rate.

Injection was performed through a 1 mm hole in the closed small side of the cell. The injection pressure was controlled by pressurizing the water reservoir. The average finger width,  $\bar{l}$ , was measured on photographs as follows. A number of straight lines (10 to 20) were drawn across the photographs, parallel to the minor axis of the cell, in order to cover regularly the whole pattern. Each intersection with fingers was then re-oriented in order to bring it more or less perpendicular to the finger axis, and all the intersection widths were averaged.

3. Finger width.

We shall successively examine the influence of cell thickness, elastic properties and injection pressure (i.e. the pressure of the water reservoir) on  $\bar{l}$ . As far as elastic properties are concerned, we will not consider the elastic modulus,  $G$ , which was not measured, but the yield stress,  $\sigma_0$ , and the Bingham yield value,  $\sigma_B$ , which in the case of an ideal Bingham fluid [10] ( $m = 1$  in Eq. (1)) would be equivalent to  $G$ .  $\sigma_0$ ,  $\sigma_B$  and  $G$  are controlled by the paste concentration,  $S/L$ . Three sets of experiments were performed, at constant  $P_i$  and  $S/L$  ( $b$  variable), constant  $P_i$  and  $b$  ( $S/L$  variable) and constant  $b$  and  $S/L$  ( $P_i$  variable).

Cell thickness ( $b$ ). — The most complete set of data was obtained with pastes at  $S/L = 0.07$  and  $P_i = 12$  kPa, i.e. in conditions where  $P_i \gg \sigma_0$ .  $b$  was varied between  $\sim 0.2$  and  $\sim 6$  mm. The set of patterns is shown in figure 3, and the  $\bar{l}$  vs.  $b$  graph is

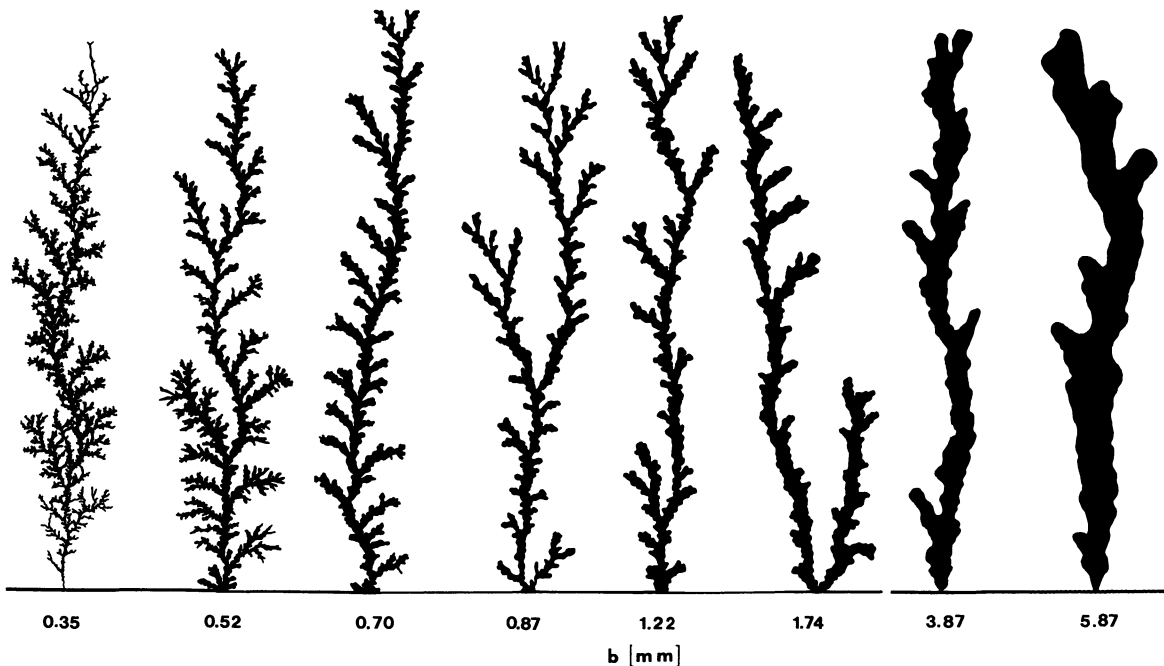


Fig. 3. — Patterns obtained by injecting water at 12 kPa in a clay paste of concentration  $S/L = 0.07$ , in cells of increasing thickness (in mm, on the figure).

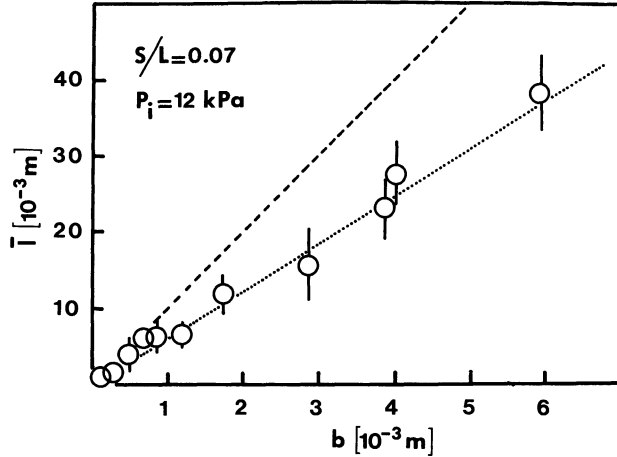


Fig. 4. — Average finger width vs. cell thickness, for the patterns of figure 3, at constant injection pressure (12 kPa) and paste concentration ( $S/L = 0.07$ ). The dashed and the dotted lines are the values predicted by equation (4) using either  $\sigma_0$  or  $\sigma_B$  as approximation for the elastic modulus.

shown in figure 4. The relationship is linear, within experimental error, with a slope of  $\sim 6.5$ :

$$\bar{l} = 6.5 b^\alpha, \quad \text{with } \alpha = 1. \quad (2)$$

A linear relationship was already observed by Daccord *et al.* [7] with polymer solutions in radial cells, in the range  $b = 0.2$  to  $b = 1.2$  mm (Fig. 4, Ref. [7]).

The finger width in miscible fingering is a point which was recently addressed by Paterson [11] and de Gennes [12]. Paterson's approach is for Newtonian viscous fluids, whereas the approach of de Gennes is for viscoelastic media. Using a viscous dissipation method, Paterson found the most rapidly growing linearly unstable wavelength,  $\lambda_m$ , to be

$$\lambda_m \approx 4 b. \quad (3)$$

This prediction is slightly below our experimental observations.

The model for viscoelastic fingering proposed by de Gennes [12] is based on the following points: (i) immediately ahead of the growing finger tips, the stress raises with a characteristic time  $\tau_S = l/U$ ; (ii) the viscoelastic medium response to this stress will be a flow only when  $\tau_S$  is longer than the viscoelastic relaxation time  $\tau_R = \mu/G$ ; (iii) the velocity of the growing tips is given by Darcy law  $U = (b^2/12\mu)|\nabla P|$ ; (iv) the pressure gradient  $|\nabla P|$  is of order  $P/l$ ; (v) the smallest wavelength for growth corresponds to  $\tau_S = \tau_R$ . Combining these conditions, one arrives at

$$l = bP^{1/2}/12 G^{1/2} \quad (4)$$

which also predicts a linear  $l = f(b)$  behaviour. Quantitatively (or semi-quantitatively), the agree-

ment of the model with the experimental values can be assessed by using the injection pressure  $P_i$  for  $P$ , and  $\sigma_0$  or better,  $\sigma_B$ , for  $G$ . Using  $\sigma_0$  leads to  $l = 11 b$  (dashed line in Fig. 4), whilst using  $\sigma_B$  leads to  $l = 6.3 b$  (dotted line), which is close to the observations.

Although satisfying, this agreement should not be overemphasized. Indeed, for concentrated suspensions like those that we used in this work, several modifications of the original model and several experimental corrections have to be introduced. Indeed, as a first modification, Darcy's law has to be replaced by

$$U \sim |\nabla P|^{1/m} \quad (5)$$

where  $m$  is the shear-thinning exponent [10]. This leads to

$$l^{(m+1)/m} = b^2 P^{1/m}/12 G. \quad (6)$$

For shear-thinning fluids with a yield stress,  $P$  in equation (6) should be replaced by  $\Delta P = P - P_0$ , where  $P_0$  is the pressure threshold for flow.  $P_0$  is clearly related to  $\sigma_0$ , but the relationship involves other parameters such as the cell thickness and the tip profile. Experimentally,  $P_0$  is not easy to measure because the flow, at pressures immediately above  $P_0$ , is extremely slow and is perturbed by mixing, diffusion and seepage phenomena [6, 9].

Harder to take into account is the fact that non Newtonian fluids are generally characterized by a broad distribution rather than by a single relaxation time.

Finally, one should be aware of the fact that the pressure in the growing finger tips,  $P$ , is smaller than the pressure in the large pressurized water reservoir where the velocity is  $\sim$  zero. In first approximation, for an horizontal cell, this pressure drop can be estimated from

$$P_i = P + \rho U^2/2 \quad (7)$$

$P_i$  is the pressure in the reservoir.  $P$  is the pressure at the finger tips growing with a velocity  $U$ .  $U$  is increasing as  $\sim (P - P_0)^{1/m}$ .

For all those reasons, the fingerwidth — cell thickness relationship does not seem to be a simple and unambiguous test for theoretical models. One fact though which seems clear and which has to be accounted for by any model is that  $l$  is a linear function of  $b$ , whether the displaced fluid has a threshold or not.

*Viscoelastic properties.* — The experiments were performed in a cell of thickness  $b = 0.35$  mm and at an injection pressure  $P_i = 104$  kPa. The paste concentration was varied from 0.06 to 0.10. This corresponds to a  $\sim$  fifty fold increase of  $\sigma_0$  (Tab. I).  $\bar{l}$  was found to decrease when  $\sigma_0$  increases, as

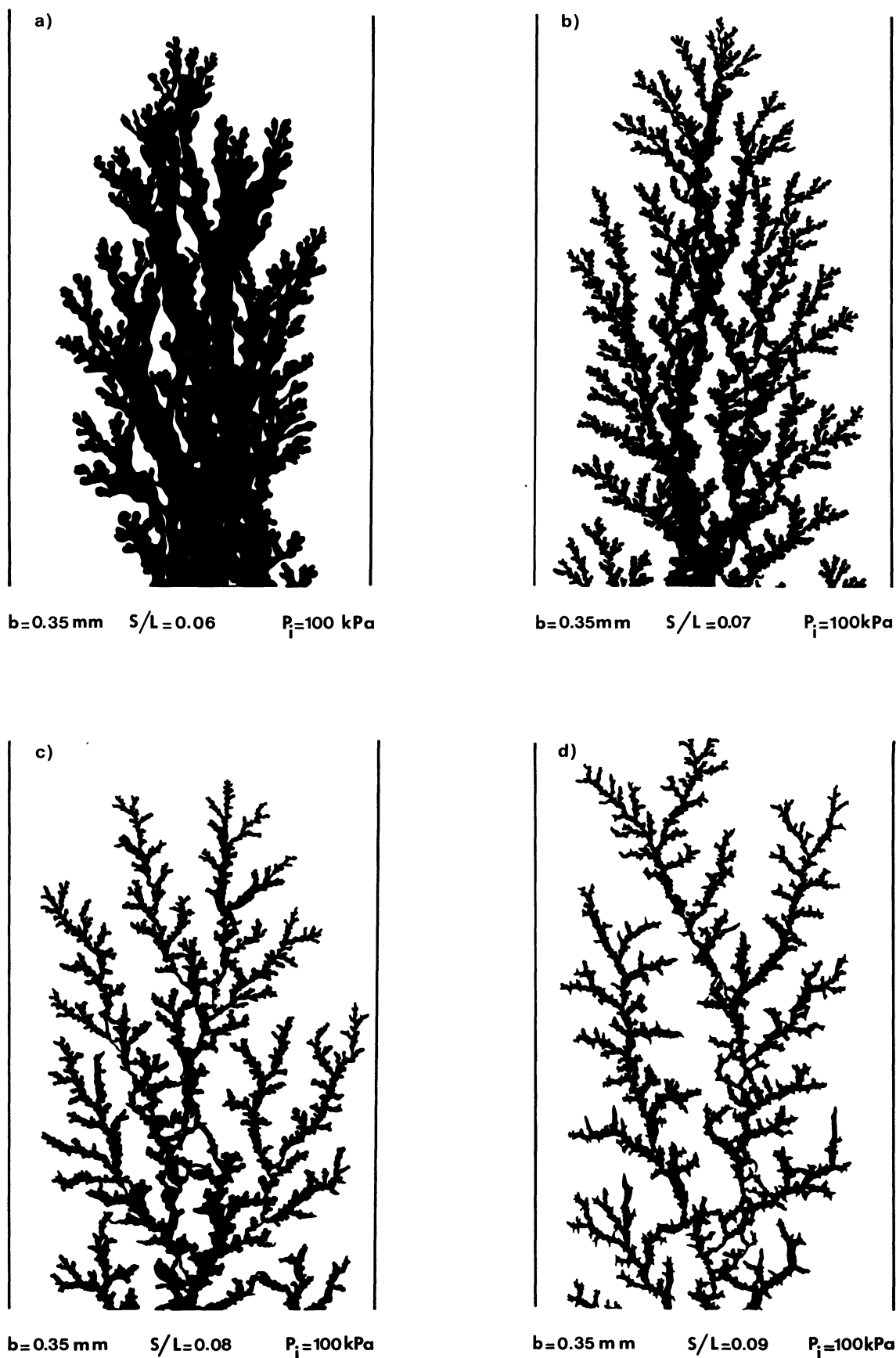


Fig. 5. — Patterns obtained by injecting water at 100 kPa in clay pastes of increasing concentration ( $S/L = 0.06, 0.07, 0.08$  and  $0.09$  in a, b, c and d, respectively), in a cell of thickness of 0.35 mm.

illustrated in figure 5. Although there is a considerable uncertainty on the  $\bar{l}$  values at low  $\sigma_0$  due to finger erosion (compare the tips and the « trunk » in Fig. 5a), the relationship seems to be of the power law type (Fig. 6) :

$$\bar{l} \sim \sigma_0^{-\beta} \tag{8}$$

with  $\beta = 0.25$ . Equation (4) predicts  $\beta = 0.50$  and equation (6), at constant  $P_0$ , would predict  $\beta = 0.29$  at  $\sigma_0 = 136$  Pa (the most concentrated paste) and  $\beta = 0.33$  at  $\sigma_0 = 3$  Pa (the least concentrated paste).

Numerically, the experimental values are well within the range predicted by equation (6) (Fig. 6).

*Injection pressure ( $P_i$ ).* — Surprisingly, increasing  $P_i$  does not lead to a concomitant increase of  $\bar{l}$ . In fact,  $\bar{l}$  decreases slightly when  $P_i$  increases, but on the other hand, the overall width of the fractal tree,  $L$ , increases significantly. In other words, the system does not respond to an increase of injection pressure by « inflating » the fingers, but by « inflating » the pattern. A set of patterns obtained at  $b = 0.52$  mm and  $S/L = 0.07$  is shown in figure 7 and the  $\bar{l}$  vs.  $P_i$  graph is shown in figure 8.

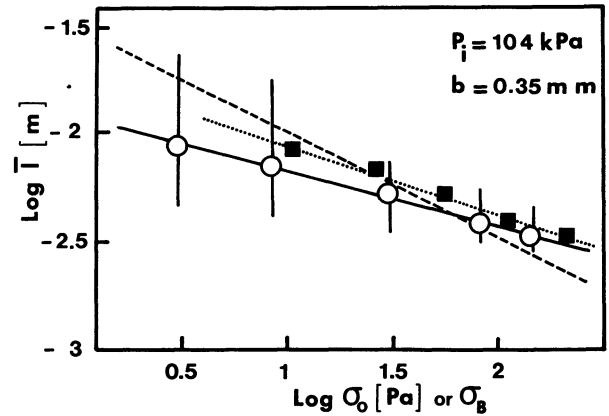


Fig. 6. — Log-Log plot of average finger width vs.  $\sigma_0$  (○, full line) or  $\sigma_B$  (■, dotted line) in a set of experiments performed at constant injection pressure ( $P_i = 100$  kPa) and constant cell thickness ( $b = 0.35$  mm). Some patterns are shown in figure 5. The dashed line is the prediction of equation (4).

This result can in no way be predicted by currently available models. There is little doubt, in view of our previous measurements in radial geometry [9], that it is a result of the increasing tip velocity which, as  $P_i$  increases, intensifies the branching cascade. In

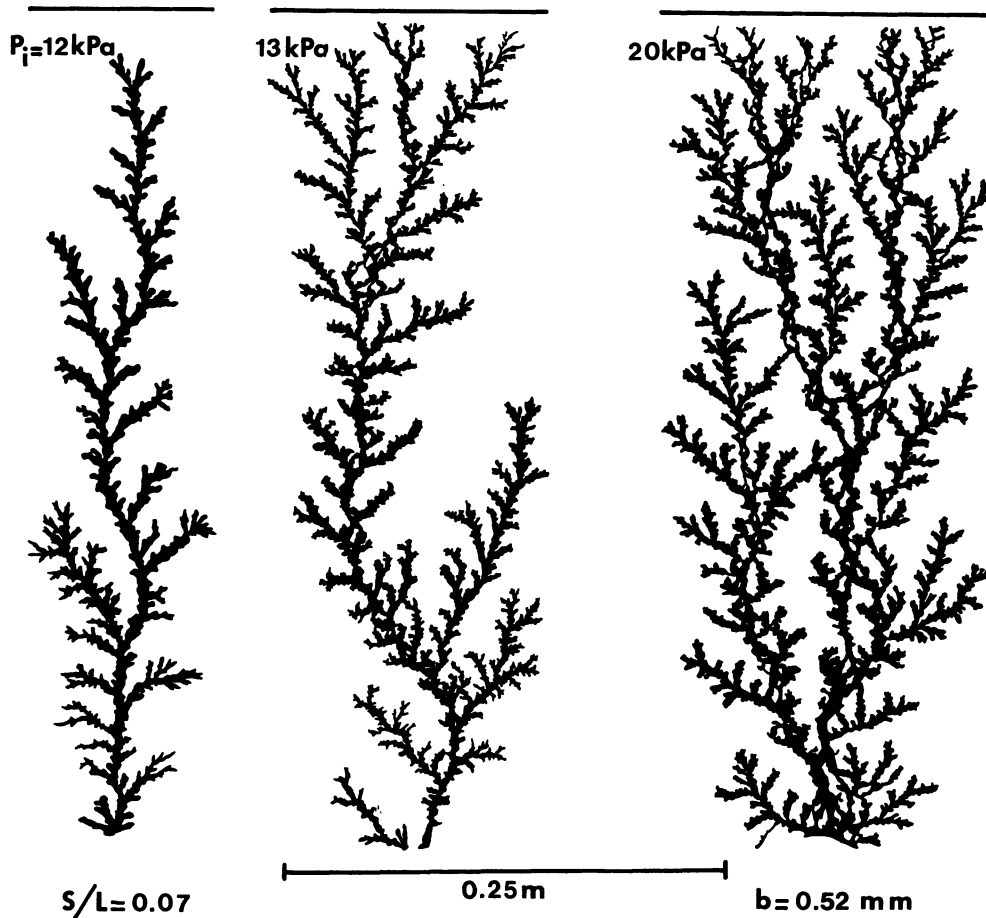


Fig. 7. — Patterns obtained by injecting water at increasing pressure ( $P_i = 12, 13$  and  $20$  kPa, respectively) in pastes of constant concentration ( $S/L = 0.07$ ) at constant cell thickness ( $b = 0.52$  mm).

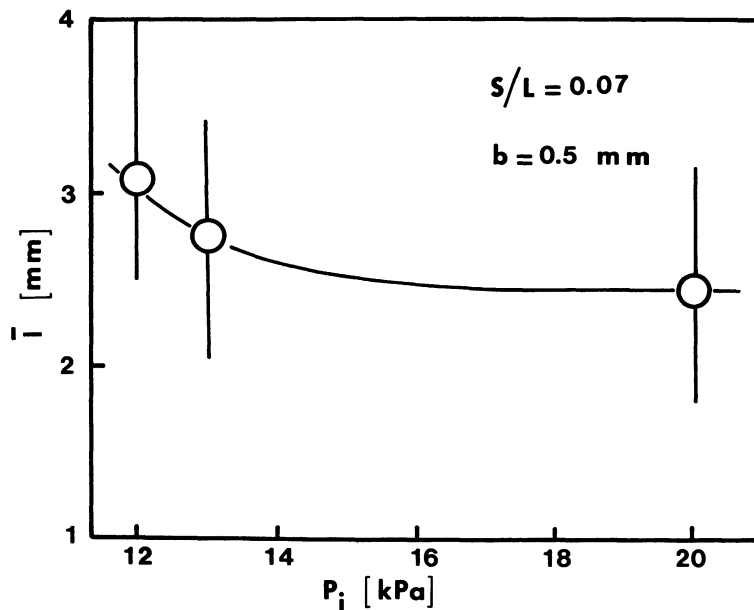


Fig. 8. — Average finger width vs. injection pressure in a set of experiments performed at constant concentration ( $S/L = 0.07$ ) and constant cell thickness ( $b = 0.52$  mm). Some patterns are shown in figure 7.

fact, it raises the fundamental question of fractal fingering. The recent findings of Nittman and Stanley [13] on the relation between fingerwidth and fluctuations in computer simulated growth suggest that understanding the role of noise would be of primary importance in this respect.

**4. Finger profile.**

The fundamental mechanism of Saffman-Taylor fingering is simple : any bump in the interface between

the low viscosity fluid and the more viscous fluid increases the pressure gradient in the more viscous fluid and tends to increase further the local velocity of the interface. This purely viscous effect is compensated to some extent by the capillary forces which tend to smooth out perturbations with small wavelength. A stability analysis leads to the consideration of a characteristic length

$$l_0 = b(T/\mu U)^{1/2} \tag{9}$$

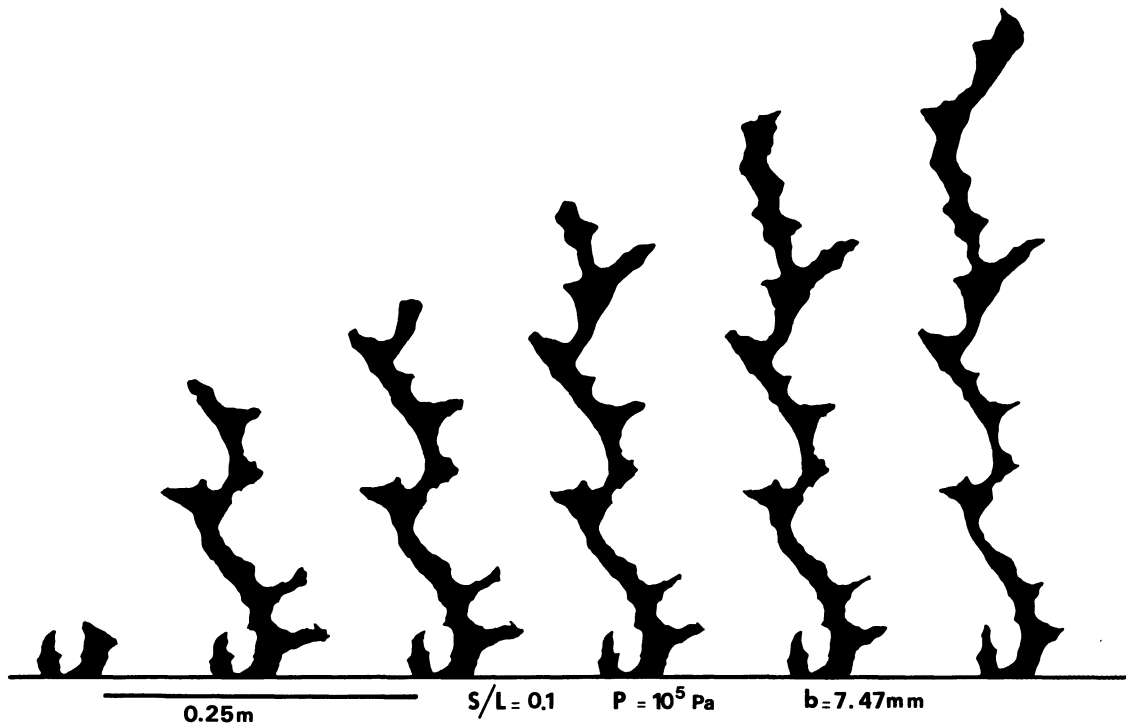


Fig. 9. — Growth sequence of a pattern obtained by injecting water at  $10^5$  Pa in a paste of concentration  $S/L = 0.1$  in a thick ( $b = 7.47$  mm) cell.



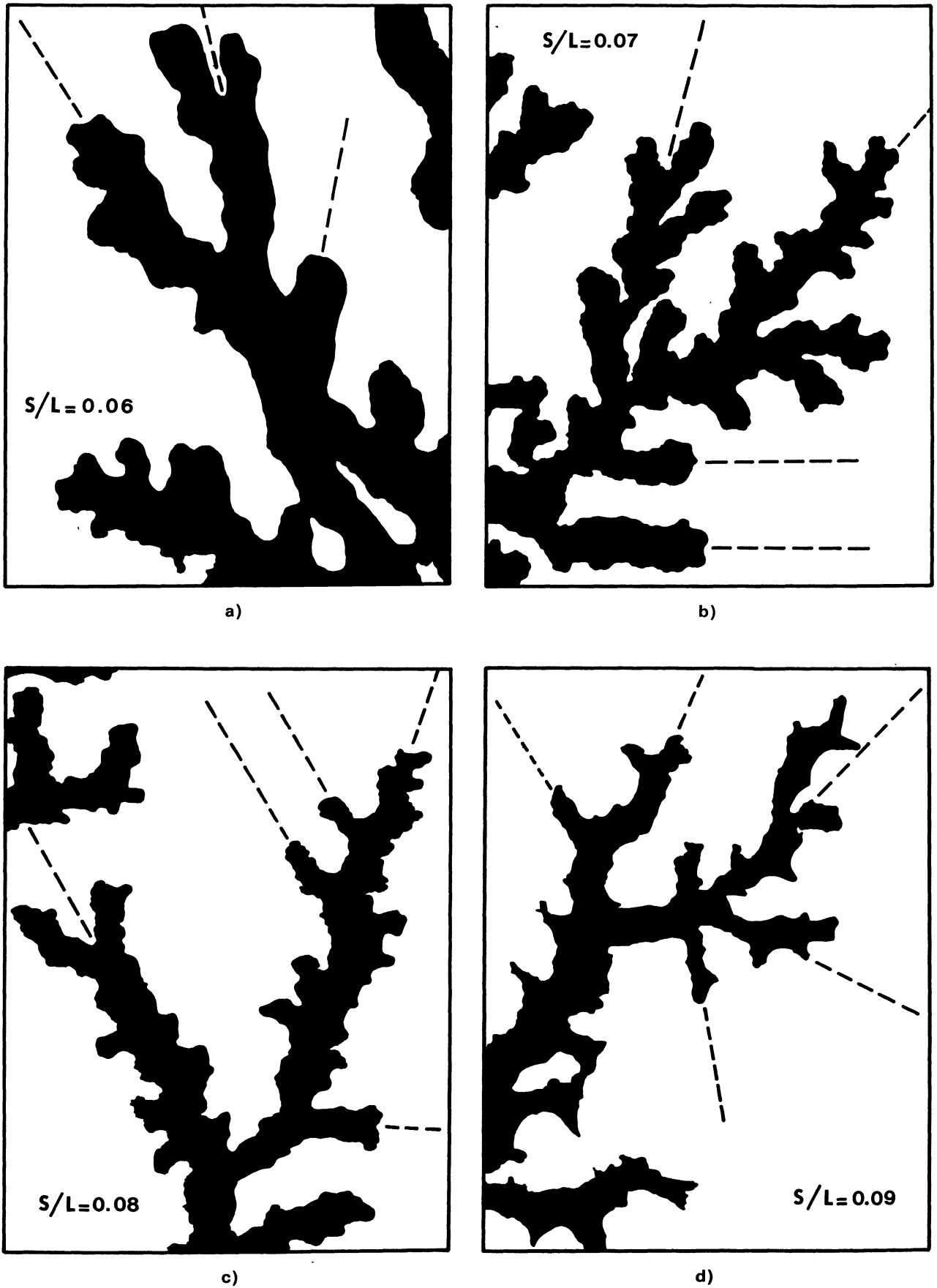
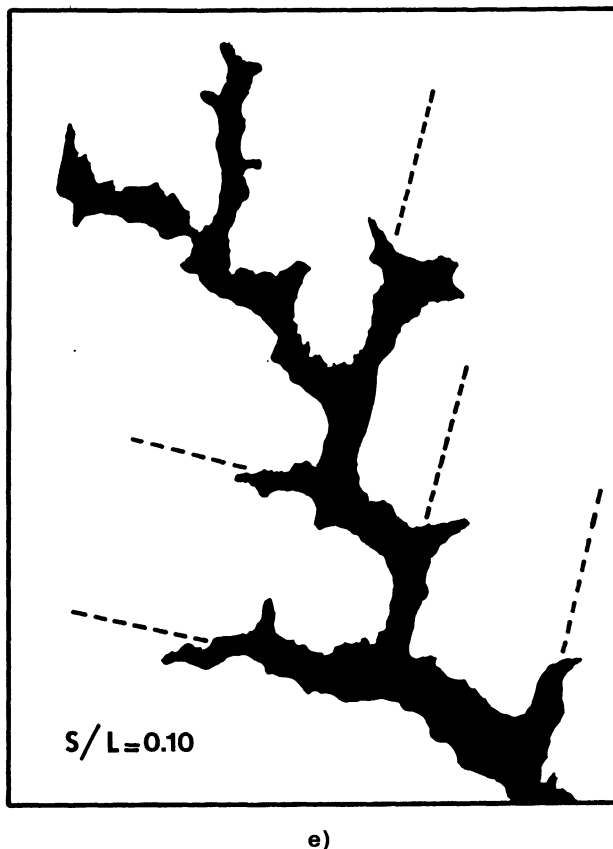


Fig. 10. — Magnifications of patterns obtained by injecting water at 100 kPa in pastes of increasing concentration ( $S/L = 0.06, 0.07, 0.08, 0.09$  and  $0.10$ , from a to e, respectively), at constant cell thickness ( $b = 0.35$  mm).



which express the ratio of capillary to viscous forces. Only those perturbations with wavelengths larger than  $\pi l_0/\sqrt{3}$  can develop. Those with smaller wavelength are smoothed out by surface tension.

For very small surface tension, the system is no longer protected against very short wavelength perturbations. Solving the dynamical equations for the interface in these conditions leads, according to initial conditions, either to finite time singularities in the form of power cusps, as shown by Shraiman and Bensimon, or to  $\lambda = 1/2$  steady fingers [14, 15]. Whilst the selection of a  $\lambda = 1/2$  finger corresponds well to Saffman-Taylor experiments, no cusp singularities have been reported yet, to our best knowledge.

*A priori*, one may think that our experimental conditions are favourable to the development of cusp instabilities. The interfacial tension between water and an aqueous paste is essentially zero, and the shear-thinning properties of the pastes are strongly destabilizing.

In actual fact, we did indeed observe cuspy finger profiles, but not in all experimental conditions: rigid pastes ( $\sigma_0 \geq 100$  Pa) are required. Fluid pastes, even at the largest tip velocities ( $U \approx 5 \times 10^{-1}$  m s $^{-1}$ ), lead only to rounded profiles (Fig. 5a for instance).

At small plate separations, the cuspy shape of the fingers is not really apparent, but leads to very

« prickly » patterns (Fig. 5d for instance). At larger separations, the small pricks become real cusps, as shown in figure 9.

Quantitatively, the cuspy character of the finger profile can be evidenced by analysing the local curvature of the finger boundary. An ideally cuspy finger would have only concave local curvatures and singular points at the tips. A smooth Saffman-Taylor finger has a convex profile at the tip, and a planar boundary along the sides. As tip splitting develops, an increasing part of the finger boundary has a concave curvature, but this merely affects the branching zones and not the tips, which remain convex.

A quantitative estimate of the cuspy character of the fingers was obtained by measuring, on a set of magnifications (Fig. 10a-e) a concavity index, defined as

$$n_{ca} = \frac{l_{ca} - l_{cx}}{l_{ca} + l_{cx}} \quad (10)$$

where  $l_{ca}$  and  $l_{cx}$  are the lengths of the boundary line regions which have a concave or convex curvature, respectively.  $l_{ca}$  and  $l_{cx}$  were measured by (i) determining visually the concave and convex curve segments of the boundary line, and (ii) measuring the total length of each set of segments with yardsticks smaller than or of the same order as the smallest wiggles on the finger profiles (Fig. 11).

As shown in figure 12,  $n_{ca}$  increases steadily with paste concentration ( $S/L$ ).  $n_{ca}$  is negative (i.e. the finger profile is predominantly convex, as in Saffman-Taylor fingers) below  $S/L = 0.08$ , and becomes positive (finger profile predominantly concave), beyond  $S/L = 0.08$ . At  $S/L = 0.10$ , 72 % of the finger boundary has a concave curvature ( $n_{ca} = 0.43$ ).

When considered as a whole, the  $n_{ca} = f(S/L)$  curve shows that an important change in curvature occurs in the same concentration range change as the sharp increase of the elastic modulus (compare Fig. 2 and Fig. 12). The change is even more dramatic when one considers only the tip profiles rather than the whole finger profiles. At  $S/L = 0.06$ , the tips are exclusively convex (Figs. 5a and 10a). At  $S/L = 0.10$ , they are almost exclusively concave (Figs. 9 and 10c).

Two mechanisms (at least) may be considered in an attempt to explain the occurrence of cusp shaped fingers: (i) the growth of cusp singularities or (ii) the onset of *fractures*. Cusp formation, as considered by Shraiman and Bensimon (SB) [14], is a purely viscous phenomenon, whereas fracture requires elastic properties. We will briefly examine the conditions in which these very different phenomena might appear.

Cusp formation, numerically evidenced by SB is a mathematical singularity which develops in very peculiar conditions. No stabilizing nor smoothing

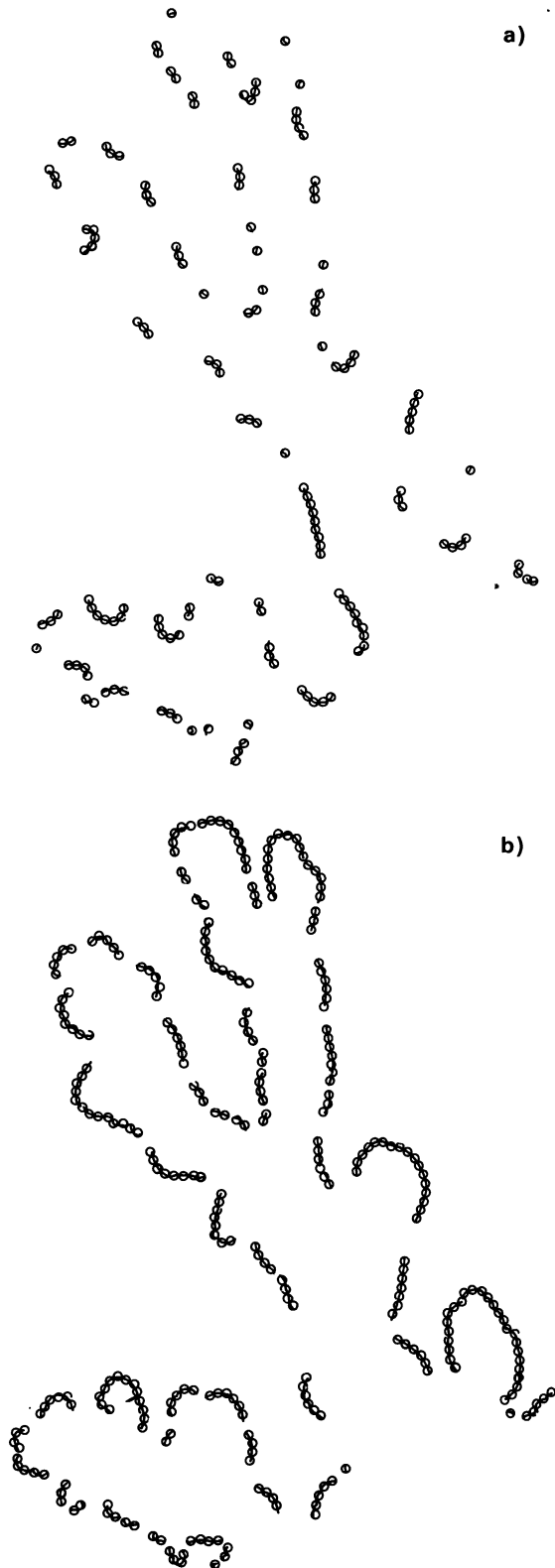


Fig. 11. — Illustration of the procedure used to measure the concave (a) and convex (b) parts of the patterns shown in figure 10.

influence has to be present. In other words, the surface tension has to be zero and, as pointed out by Nittmann and Stanley [13], the system should be free of noise. Only in those conditions will a small

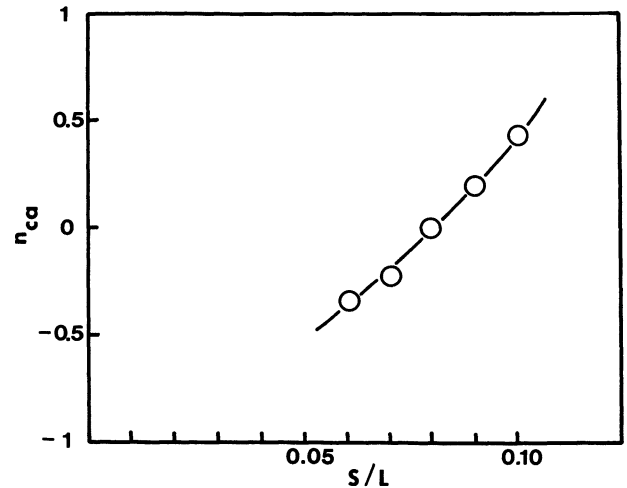


Fig. 12. — Concavity index (defined in text, Eq. (10)) vs. paste concentration, in a set of experiments performed at constant injection pressure ( $P_i = 100$  kPa) and cell thickness ( $b = 0.35$  mm) (Figs. 5 and 10).

perturbation of the interface between a viscous fluid and a less viscous fluid sharpen to a point where the tip curvature and the tip curvature become essentially infinite.

As far as the cusp shaped fingering that we observed corresponds to the appearance of a real cusp singularity, it raises at least two questions: (i) why does it stop after a while or, more exactly, why is it restricted to the tips and why to *fingers* continue to grow? (ii) why does it only happen in the more concentrated pastes, or in other words, why would the sources of noise decrease with concentration and why does everything happen as if the interface tension between a solvent (water) and a dispersion of colloidal particles in the same solvent were *decreasing* as the concentration of the dispersion increases. We see no obvious answer to the first question. There is indeed no doubt that cusps are soon relayed by fingers, as shown in figure 13, in which a radial cuspy pattern obtained in a concentrated paste is compared with a SB-type pattern. This is in fact a strong argument against an explanation of our observations in terms of cusp singularities. On the other hand, the second question can be approached by considering the physical meaning of the interface tension in miscible viscoelastic media.

Thermodynamically the interfacial tension  $T$  is defined as the partial derivative of the system free enthalpy with respect to interface area,  $A$ , at constant pressure, temperature ( $\theta$ ) and composition ( $C$ ), *at thermodynamic equilibrium*. The latter condition is easily met at the interface between immiscible fluids, but can obviously not be met with miscible fluids without destroying the interface, unless, for some reason, the fluids do not mix. Such a reason might be the existence of a threshold for flow ( $\sigma_0$ ). In the region where  $\sigma < \sigma_0$  the system would

behave as a phase-separated fluid-solid mixture with zero interface tension and a well defined and stable concentration profile would build up at the interface. However, this is unlikely to happen at the tips, where the stress is maximum. Thus, one is left with the problem of explaining why an (effective) interface tension might build up between a viscoelastic medium and a miscible solvent, even above  $\sigma_0$ .

The same problem has to be faced if one explains the cusp shaped fingers in the more concentrated pastes in terms of fracture or, more exactly, in terms of subcritical crack growth [16]. Crack propagation in viscoelastic solids (elastomers for instance) is described by the following equation [17]

$$g - 2 T = 2 T \phi (U) \tag{11}$$

$g$  is the strain energy release rate and  $T$  is the intrinsic surface energy, i.e. the water-paste interface tension in the present case.  $\phi$  is a velocity ( $U$ ) dependent term which is related to viscoelastic losses or internal friction at the crack tip. It is clear from equation (11) that this type of model breaks down for  $T = 0$ .

**5. Branching angle and finger stability.**

The last point on which we would like to report some data is the tip splitting angle which, just like the finger and tip curvature, undergoes deep modifications as the paste rigidity increases. As illustrated in figure 10a-e and plotted in figure 14, the average branching angle goes from  $\sim 25^\circ$  at  $S/L = 0.06$  to  $\sim 85^\circ$  at  $S/L = 0.10$ . Thus, the branching geometry of the pattern goes from almost parallel branching (as in a Chandler) to perpendicular branching, in the same concentration range where the curvature transition takes place.

Branching angles in natural patterns (trees, rivers) are usually interpreted in terms of the principle of least work, which states that the length of the branches and their angles in a pattern are such as to minimize the work of pressure forces [18]. Thus, a narrow side branch will split off from the main branch at close to a 90-degree angle because this minimizes the work of the pressure driving the fluid in the narrow branch. On the other hand, if the main and side branches are close to the same size, the fluid will, with little difficulty, switch over to the side branches and such side branches will strike off from the main branch at angles considerably narrower than 90 degrees.

The principle of least work does not seem to apply in the present case. In each pattern, the branching angle is statistically independent of finger width and length. Actually, we feel that this is but a consequence of the fact that the viscosity of the fluid within the finger is negligible with respect to that of the displaced medium. In other words, there is no load drop within the fingers.

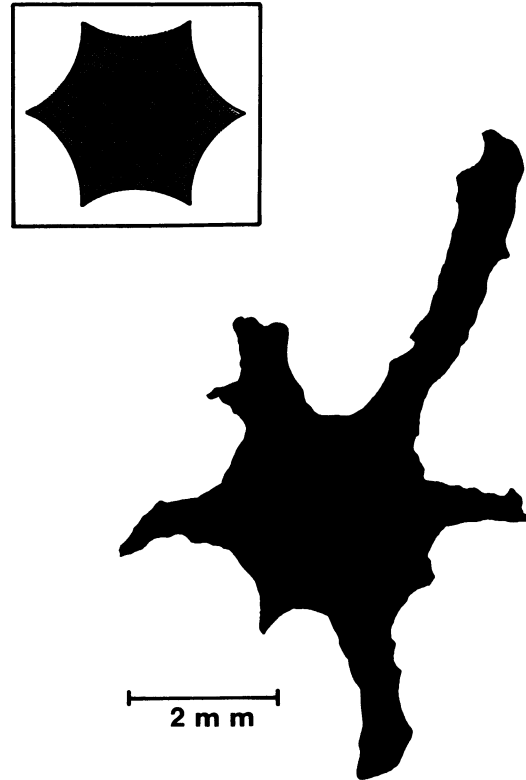


Fig. 13. — Pattern obtained by injecting water at  $10^5$  Pa in a paste of concentration  $S/L = 0.1$ , in a radial cell ( $b = 5$  mm). The size of the injection hole (1 mm) is  $\sim$  three times smaller than the large central spot. The insert shows a cuspy interface generated by numerical simulation (adapted from Ref. [14]).

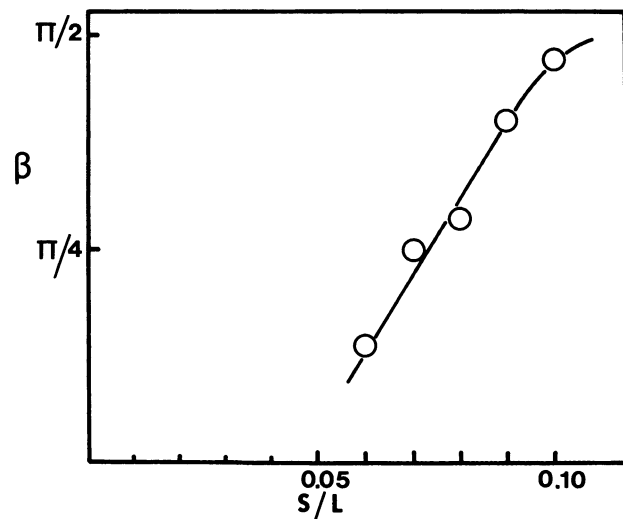


Fig. 14. — Average branching angle as a function of paste concentration in a series of experiments performed at constant injection pressure ( $P_i = 100$  kPa) and cell thickness ( $b = 0.35$  mm) (Fig. 10).

However, it should be pointed out that this is not a guarantee that the pressure is homogeneous within the fingers or, equivalently, that the finger boundary

is an equipotential surface. It is obvious from figures 5 and 10 that a finger is actually a sequence of swelling and necks, and even the simple flow of a non viscous fluid in such an inhomogeneous pipe should lead to pressure inhomogeneities.

In fact, the most relevant experimental observations which might help us understanding the branching behaviour are the following : (i) the opening of the branching angle — as well as the change in finger profile — occurs in a concentration range where the elastic properties of the embedding medium develop. 90° branching — as well as cusps — is observed at a point where the elastic modulus undergoes such a rapid rise that a sol-gel transition seems to be impending ; (ii) branching is far from being always symmetrical (symmetrical branching being defined as the splitting of a finger into two equal fingers making the same angle with the axis of the parent finger). As far as one can judge from the patterns in figure 10a-e, branching is close to symmetrical in the more fluid pastes, but becomes increasingly asymmetrical as the paste gets more rigid. At  $S/L = 0.10$ , the branching cascade of the pattern has a very asymmetrical staircase-like structure (Fig. 9 is very illustrative), with several flights of stairs in which each stair is a totally asymmetric disturbance with respect to the axis of the flight ; (iii) in all patterns, the finger sides are covered by asymmetrical bumps or cusps which may be considered as the buds of side branches which will never grow further. Growth is indeed restricted to the unscreened front regions of the pattern, in which the pressure gradient (towards the exit of the cell) is the largest [7, 9].

The symmetry of the disturbances of Saffman-Taylor fingers is a point which was addressed by Bensimon *et al.* [15]. Several unstable modes were predicted, two of them being observed experimentally : the symmetrical tip-splitting mode, already observed by Park and Homsy [3] and the asymmetrical « hump » mode, recently observed by Tabeling, Zocchi and Libchaber [3]. The evolution of a hump is interesting. It starts as an asymmetrical hernia of the finger tip. As the finger moves forward, it is repelled on the side of the finger where the velocity is slower and finally vanishes as it goes away from the tip.

When taken together, our observations and those of Tabeling *et al.* [3] suggest that the opening of the branching angle might be due to a progressive takeover of the branching mechanism by asymmetrical modes, which may be either hump or cusp modes according to the paste concentration.

Similarly to what happens for the finger profile, the opening of the branching angle might also be

explained in terms of crack growth. If the finger (or crack) tip grows at a velocity larger than  $l/\tau_R$ , then a stress will develop *behind* the tip, along the finger. This stress will be oriented parallel to the finger and will grow as the tip moves forward. At some point, a lateral crack could grow and relax the stress. The orientation of this crack will naturally be at 90° with respect to the main finger. As the tip keeps moving, the lateral stress will grow again and a second lateral crack would form, and so on. This might explain the quasi-periodicity of lateral branching in figure 9, for instance.

The main difference between the hump mode and the lateral crack mechanism is that in the later case, branching would start *behind* the tip whereas in the former case, it would start at the tip and then slide along the main finger. This might provide an experimental method for deciding which mechanism is actually operating.

## 6. Conclusion.

All the data reported in this paper point to one major but yet qualitative conclusion : *viscoelastic effects are of primary importance in fingering between miscible fluids*. The elastic properties of the more viscous fluid control to a large extent the width of the fingers and their profile, and perhaps also their branching angle. However, the relative insensibility of the *finger* width and, conversely, the sensibility of the *pattern* width to injection pressure have still to be understood.

The most serious problem, about which our data raise as many questions than they do provide answers, is the branching mechanism which is itself controlled by the type of disturbance generated by the finger tip. Even simple (but fundamental) questions such as the relative importance of flow and fracture phenomena are still totally open. A clue, which is worth being tested further, is that the stress rise time might undergo fluctuations around the  $\tau_S = \tau_R$  condition. If this happens to be true, then one would expect pressure and velocity fluctuations within the finger. This is currently tested in our laboratory.

## Acknowledgments.

We would like to thank P. G. de Gennes for giving to us a draft of his paper (Ref. [12]) and for triggering the idea that the stress rise time,  $\tau_S$ , may be in many instances close to the viscoelastic relaxation time,  $\tau_R$ . One of the referees is also acknowledged for pointing to us some difficulties of the cusp singularity model.

## References

- [1] SAFFMAN, P. G. and TAYLOR, G. I., *Proc. Roy. Soc. A* **245** (1958) 312.
- [2] NITTMANN, J., DACCORD, G. and STANLEY, H. E., *Nature* **314** (1985) 141.
- [3] WOODING, R. A., *J. Fluid Mech.* **39** (1969) 477 ;  
 GUPTA, S. P., VARNON, J. E. and GREENKORN, R. A., *Water Resour. Res.* **9** (1973) 1039 ;  
 WHITE, I., COLOMBERA, P. M. and PHILIP, J. R., *Soil Sci. Soc. Am. J.* **40** (1976) 824 ;  
 PITTS, E., *J. Fluid Mech.* **97** (1980) 53 ;  
 MAHER, J. V., *Phys. Rev. Lett.* **54** (1984) 1498 ;  
 TABELING, P. and LIBCHABER, A., *Phys. Rev. A* **33** (1986) 794 ;  
 TABELING, P., ZOCCHI G. and LIBCHABER, A., *J. Fluid Mech.*, in press ;  
 PARK, C. W., GORELL, S. and HOMSY, G. M., *J. Fluid Mech.* **141** (1984) 275 ;  
 PARK, C. W. and HOMSY G. M., *Phys. Fluids* **28** (1985) 1583 ;  
 PATERSON, L., *J. Fluid Mech.* **113** (1981) 513.
- [4] CHUOKE, R. L., VAN MEURS, P. and VAN DER POL, *Trans. AIME* **216** (1959) 188 ;  
 TRYGGVASON, G. and AREF, H., *J. Fluid Mech.* **136** (1983) 1 and **154** (1985) 287 ;  
 MCLEAN, J. W. and SAFFMAN, P. G., *J. Fluid Mech.* **102** (1981) 455 ;  
 PARK, C. W. and HOMSY, G. M., *J. Fluid Mech.* **139** (1984) 291 ;  
 VANDENBROECK, J. M., *Phys. Fluids* **26** (1983) 2033 ;  
 KESSLER, D. and LEVINE, H., *Phys. Rev. A* **33** (1986) 3352 ;  
 SHRAIMAN, B., *Phys. Rev. Lett.* **56** (1986) 2028 ;  
 HONG, D. C. and LANGER, J. S., *Phys. Rev. Lett.* **56** (1986) 2032 ;  
 COMBESCOT, R., PUMIR, A., POMEAU, Y., DOMBRE, T. and HAKIM, V., *Phys. Rev. Lett.* **56** (1986) 2036.
- [5] DACCORD, G., NITTMANN, J. and STANLEY, H. E., in *On Growth and Form*, H. E. Stanley and N. Ostrowsky Eds. (Martinus Nijhoff Pub., Boston) 1986, p. 203-210.
- [6] STANLEY, H. E., DACCORD, G., HERRMANN, H. J. and NITTMANN, J., in *Scaling Phenomena in Disordered Systems*, R. Pynn and A. Skjeltop Eds., NATO ASI Series, **B 133** (Plenum Press, New York) 1985, p. 85-97.
- [7] DACCORD, G., NITTMANN, J. and STANLEY, H. E., *Phys. Rev. Lett.* **56** (1986) 336.
- [8] VAN DAMME, H., OBRECHT, F., LEVITZ, P., GATINEAU, L. and LAROCHE, C., *Nature* **320** (1986) 731.
- [9] VAN DAMME, H., LAROCHE, C. and GATINEAU, L., *Revue Phys. Appl.* **22** (1987) 241.
- [10] For instance : BIRD, R. B., ARMSTRONG, R. C. and HAFFAGER, D., *Dynamics of Polymeric Liquids* (Wiley, New York) (1977).
- [11] PATERSON, L., *Phys. Fluids* **28** (1985) 26.
- [12] DE GENNES, P. G., *Europhys. Lett.* **3** (1987) 195.
- [13] NITTMANN, J. and STANLEY, H. E., *Nature* **321** (1986) 663.
- [14] SHRAIMAN, B. and BENSIMON, D., *Phys. Rev. A* **30** (1984) 2840.
- [15] BENSIMON, D., KADANOFF, L. P., LIANG, S., SHRAIMAN, B. I. and TANG, C., *Rev. Mod. Phys.*, in press.
- [16] MAUGIS, D., *J. Mater. Sci.* **20** (1985) 3041.
- [17] MAUGIS, D. and BARQUINS, M., *J. Phys. D : Appl. Phys.* **11** (1978) 1989.
- [18] MURRAY, C. D., *J. Gen. Physiol.* **9** (1926) 835 and **10** (1927) 725, cited by STEVENS, P. S. in *Patterns in Nature* (Little, Brown and Company, Boston) 1974, and by D'ARCY THOMPSON in *On Growth and Form*, abridged edition ed. by J. T. Bonner (Cambridge Univ. Press, Cambridge) 1984.
-